International Symposium on Biomedical Imaging
(ISBI) 2004

LARGE DEFORMATION MINIMUM MEAN SQUARED ERROR TEMPLATE ESTIMATION FOR COMPUTATIONAL ANATOMY

Brad Davis, Peter Lorenzen, and Sarang Joshi

MIDAG
University of North Carolina, Chapel Hill
{davisb, lorenzen, joshi}@cs.unc.edu

ABSTRACT

This paper presents a method for large deformation exemplar template estimation. This method generates a representative anatomical template from an arbitrary number of topologically similar images using large deformation minimum mean squared error image registration. The template that we generate is the image that requires the least amount of deformation energy to be transformed into every input image. We show that this method is also useful for image registration. In particular, it provides a means for inverse consistent image registration. This method is computationally practical; computation time grows linearly with the number of input images. Template estimation results are presented for a set of five 3D MR human brain images.

1. INTRODUCTION

Computational anatomy is the study of anatomical variation. For a set of images representing some population, a natural problem in computational anatomy is the construction of an exemplar template—an image that serves as a representative for the population. Such a template must represent the anatomical variation present in the images [1, 2, 3, 4].

The construction of anatomical templates is inherently related to the construction of transformations that map one anatomy to another. Various transformation groups have been studied for image mapping. These groups vary in dimensionality from simple global translations ($\Re^3$) and rigid rotations ($SO(3)$) to the infinite dimensional group of diffeomorphisms ($\mathcal{H}$) [4].

The optimal anatomical representation is one that requires the 'minimum amount of transformation' from the template to each of the anatomical images. For low dimensional transformation groups, the Procrustes method produces such a template [5]. In the small deformation high dimensional setting one can build a template by averaging registration maps [1]. This averaging approach is not valid in the large deformation diffeomorphic setting since the sum of diffeomorphic transformations is not guaranteed to be a diffeomorphism. In this paper we develop a methodology for building exemplar templates from a population of anatomical images in the large deformation diffeomorphic setting.

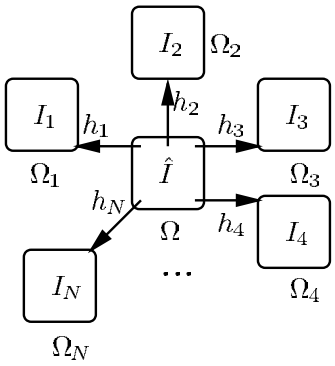

Fig. 1. Template Construction Framework

2. EXEMPLAR TEMPLATES

We consider the problem of estimating a template image $\hat{I}$ that is the best representative for a population of N anatomical images $\{I_i\}_{i=1}^N$. $\hat{I}$ need not be a member of $\{I_i\}$. To this end, we consider the problem of constructing a mapping between $\hat{I}$ and each image in the set $\{I_i\}$. That is, we would like to find the mappings $h_i : \Omega \rightarrow \Omega_i$ where $\Omega \subset \Re^3$ and $\Omega_i \subset \Re^3$ are the coordinate systems of the images $\hat{I}$ and I_i respectively. Ω is independent of any of the input image coordinate systems. This framework is depicted in Figure 1.

Given a metric on a group of transformations, we seek the representative template image $\hat{I}$ that requires the minimum amount of energy to deform into every population image I_i. More precisely, given a transformation group $\mathcal{S}$ with associated metric $D : \mathcal{S}^2 \rightarrow \Re$, along with an image

dissimilarity metric $E(I_1, I_2)$, we wish to find the image $\hat{I}$ such that

$$\{\hat{h}_i, \hat{I}\} = \underset{h_i \in \mathcal{S}, I}{\operatorname{argmin}} \sum_{i=1}^{N} E(I_i \circ h_i, I) + D(e, h_i) \quad (1)$$

where e is the identity transformation.

In this paper we focus on the infinite dimensional group of diffeomorphisms $\mathcal{H}$. We apply the theory of large deformation diffeomorphisms [6, 7] to generate deformations $h \in \mathcal{H}$ that are solutions to the Lagrangian ODEs $\frac{d}{dt}h(x,t) = v(h(x,t),t)$. The transformations h are generated by integrating velocity fields v forward in time. Inverse transformations h_i^{-1} are generated by integrating the negative velocity fields $\tilde{v}$ backwards in time. The relationship between v and $\tilde{v}$ is given by $v(h(x,t),t) = -\tilde{v}(\phi(y, 1-t), 1-t)$. This relationship is shown in Figure 2. The location y is described in terms of the forward integration of the velocity field v starting from the location x. Similarly, x can be described in terms of integrating the negative velocity field $\tilde{v}$ backwards in time starting at y.

We induce a metric on the space of diffeomorphisms by using a Sobolov norm via a partial differential operator L on the velocity fields v. Let h be a diffeomorphism isotopic to the identity transformation e. We define the distance $D(e,h)$ as

$$D(e,h) = \min_{v} \int_0^1 \int_\Omega ||Lv(x,t)||^2 \, dxdt$$

subject to

$$h(x) = \int_0^1 v(h(x,t),t)\, dt.$$

The distance between any two diffeomorphisms is defined by

$$D(h_1, h_2) = D(e, h_1^{-1} \circ h_2).$$

This distance satisfies all of the properties of a metric [8]. Namely it is non-negative, symmetric, and satisfies the triangle inequality. D is trivially non-negative. Symmetry follows from the fact that h^{-1} is generated by integrating backwards in time the negative of the velocity field that generates h. Hence the minimizer of Equation 2 is the same for both h and h^{-1}, implying that $D(e,h) = D(e,h^{-1})$. Miller et al. [7] give a detailed discussion of D and show that it satisfies the triangle inequality.

3. LARGE DEFORMATION TEMPLATE CONSTRUCTION

Having defined a metric on the space of diffeomorphisms, the minimum energy template estimation problem (Equation 1) is formulated as

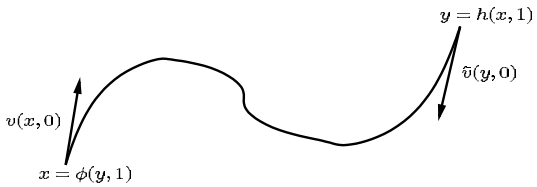

Fig. 2. Velocity Field Integration

$$\{\hat{h}_i, \hat{I}\} = \underset{h_i, I}{\operatorname{argmin}} \sum_{i=1}^{N} E(I_i \circ h_i, I) + \int_0^1 \int_\Omega ||Lv_i(x,t)||^2 \, dxdt$$
$$\text{subject to: } h_i(x) = \int_0^1 v_i(h_i(x,t),t)\, dt. \quad (2)$$

Throughout this paper we use the squared error dissimilarity metric but other metrics such as the Kullback-Leibler divergence can also be used [9]. Under the squared error dissimilarity measure the template estimation problem becomes

$$\{\hat{h}_i, \hat{I}\} = \underset{h_i, I}{\operatorname{argmin}} \sum_{i=1}^{N} \int_\Omega \left(I_i\left(h_i\left(x\right)\right) - I(x)\right)^2 dx + \int_0^1 \int_\Omega ||Lv_i(x,t)||^2 \, dxdt. \quad (3)$$

This minimization problem can be simplified by noticing that for fixed transformations h_i, the $\hat{I}$ that minimizes Equation 3 is given by

$$\hat{I}\left(x\right) = \frac{1}{N} \sum_{i=1}^{N} I_i\left(h_i\left(x\right)\right). \quad (4)$$

In words, $\hat{I}$ is the voxelwise arithmetic mean of the deformed images $I_i\left(h_i\left(x\right)\right)$. Note that the method for computing $\hat{I}$ from $\{I_i\}$ is determined by the image dissimilarity metric used. Other image dissimilarity metrics would imply different methods for computing $\hat{I}$.

Combining Equations 3 and 4 results in

$$\hat{h}_i = \underset{h_i}{\operatorname{argmin}} \sum_{i=1}^{N} \int_\Omega \left(I_i\left(h_i\left(x\right)\right) - \frac{1}{N} \sum_{j=1}^{N} I_j\left(h_j\left(x\right)\right) \right)^2 dx + \int_0^1 \int_\Omega ||Lv_i(x,t)||^2 \, dxdt. \quad (5)$$

Note that the solution to this minimization problem is independent of the ordering of the N images.

This template construction framework produces transformations $\hat{h}_i$ such that $\hat{h}_i : \Omega \rightarrow \Omega_i$. Since each $\hat{h}_i$ is a diffeomorphism, its inverse $\hat{h}_i^{-1} : \Omega_i \rightarrow \Omega$ exists and can be calculated by integrating the negative velocity fields backwards in time (Figure 2). Image to image correspondences can be computed from these transformations using the composition rule

$$\hat{h}_{i,j} = \hat{h}_j \circ \hat{h}_i^{-1} : \Omega_i \rightarrow \Omega_j. \quad (6)$$

4. INVERSE CONSISTENT IMAGE REGISTRATION

When the template construction framework presented in the previous section is applied to two images the result is an inverse consistent image registration algorithm.

A registration framework is inverse consistent if image ordering does not affect the registration result. Many image registration algorithms are not inverse consistent because their image dissimilarity metrics are computed in the coordinate system of one of the images being registered. The choice of such a reference image can bias the result of the registration. Inverse consistent registration is desired when there is no *a priori* reason to choose one image over another as a reference image. Previous work (e.g. [10]) has introduced methods for computing approximate inverse consistent registrations by applying inverse consistency constraints on intermediate incremental transformations. The framework presented here leads to an inherently inverse consistent image registration—no correction penalty for consistency is required.

For two images I_1 and I_2, Equation 5 reduces to

$$\{\hat{h}_1, \hat{h}_2\} = \underset{h_1,h_2}{\operatorname{argmin}} \frac{1}{2} \int_\Omega \left(I_1\left(h_1\left(x\right)\right) - I_2\left(h_2\left(x\right)\right)\right)^2 dx + \int_0^1 \int_\Omega \left\|Lv_1(x,t)\right\|^2 dxdt + \int_0^1 \int_\Omega \left\|Lv_2(x,t)\right\|^2 dxdt.$$

The transformations h_1 and h_2 map Ω to Ω_1 and Ω_2 respectively. Using the composition rule (Equation 6), we define the transformations $h_{1,2} : \Omega_1 \rightarrow \Omega_2 = h_2 \circ h_1^{-1}$ and $h_{2,1} : \Omega_2 \rightarrow \Omega_2 = h_1 \circ h_2^{-1}$. In other words, $h_{1,2}$ is a transformation from I_1 to I_2 and $h_{2,1}$ is a transformation from I_2 to I_1. This method is inverse consistent since $h_{1,2} \circ h_{2,1} = h_{2,1} \circ h_{1,2} = e$, the identity transformation.

5. IMPLEMENTATION

Following Christensen's algorithm for propagating templates described in [11, 6], we approximate the solution to the minimization problem in Equation 5 using an iterative greedy method. At each iteration k, the updated transformation h_i^{k+1}, for each image I_i, is computed using the update rule $h_i^{k+1} = h_i^k\left(x + \varepsilon v_i^k(x)\right)$. h_i^k and v_i^k are the current estimated transformation and velocity for the ith image, and ε is the step size. In other words, each final transformation h_i is built up from the composition of k transformations.

The velocity v_i^k for each iteration k is computed as follows. First, compute the updated template estimate

$$\hat{I}^k(x) = \frac{1}{N} \sum_{i=1}^{N} I_i^k(x),$$

where $I_i^k = I_i(h_i^k(x))$ is the i^{th} image deformed by h_i^k. Next, define force functions

$$F_i^k(x) = -\left[I_i^k(x) - \hat{I}^k(x)\right] \nabla I_i^k(x).$$

This is the variation of the image dissimilarity term in Equation 5 with respect to h_i. The velocity field v_i^k is computed at each iteration by applying the inverse of the differential operator L to the force function, i.e. $v_i^k(x) = L^{-1} F_i^k(x)$, where $L = \alpha\nabla^2 + \beta\nabla\cdot\nabla + \gamma$ is the Navier-Stokes operator. This computation is carried out in the Fourier domain [12].

For each iteration the dominating computation is the Fast Fourier Transform. Thus, the order of the algorithm is $MNn \log n$ where M is the number of iterations, N is the number of images to be registered, and n is the number of voxels in each image. The complexity increases only linearly as images are added, making the algorithm extremely scalable. Satisfactory correspondence is typically achieved after 200 iterations. In practice, we use a multi scale approach that initializes the fine (voxel) scale registration with the upsampled correspondence computed at a coarser scale level. The finer scale levels only need to account for residue from coarser scale levels and thus require far fewer iterations to converge.

6. RESULTS

To evaluate the performance of this method we applied our algorithm to a set of five 176x156x192 intensity adjusted 3D MR brain images taken from five different subjects. As a preprocessing step, these images were aligned using a similarity transform. An axial slice from each of these initial images is shown in the first column of Figure 3. There is noticeable large deformation variation between these anatomies. The second column of Figure 3 shows the deformed (3D) images after 500 iterations of our algorithm. The deformed images look very similar, as they have been deformed into the common coordinate space of the template.

Figure 4 shows the initial and final estimate of the template. The initial template estimate is blurry since it is an average of the the varying individual neuroanatomies. Ghosting is evident around the lateral ventricles and the near the

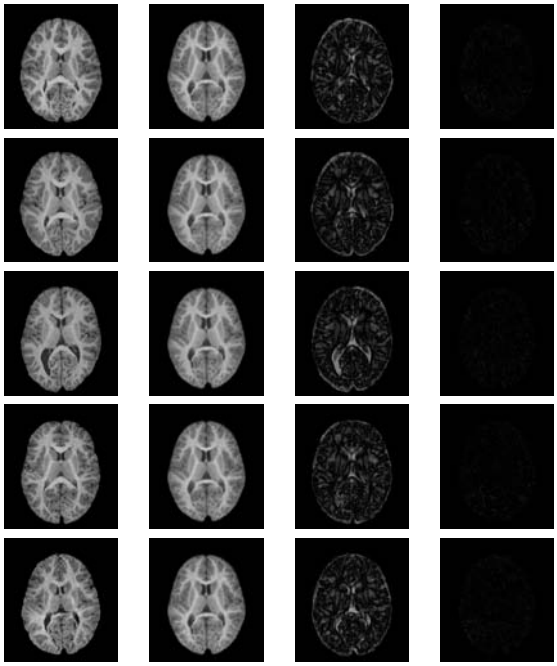

Fig. 3. Template Construction. Column 1 shows the initial images. Column 2 shows the deformed images after 500 iterations. Column 3 shows the absolute error between the initial images and the initial template estimate. Column 4 shows the absolute error between the deformed images and the final template estimate.

boundary of the brain. Column 3 of Figure 3 shows the absolute error between each input image and the initial template estimate. After applying our algorithm the deformed neuroanatomies are nearly identical, resulting in a sharp final template estimate. Column 4 of Figure 3 shows the absolute error between each deformed image and the final template estimate. The final template estimate is nearly identical to each of the deformed neuroanatomies.

7. ACKNOWLEDGMENTS

The authors would like to thank Guido Gerig for supplying the MR brain images used in our experiments, Matthieu Jomier for his work in producing results for this paper, and Theodore Kim for his helpful suggestions on improving this manuscript. This work was supported by NIBIB-NIH grant R01 EB000219, DOD Prostate Cancer Research Program DAMD17-03-1-0134, the UNC-Schizophrenia Research Center, and the NIMH Silvio Conte Center for the Neuroscience of Mental Disorders (MH64065).

8. REFERENCES

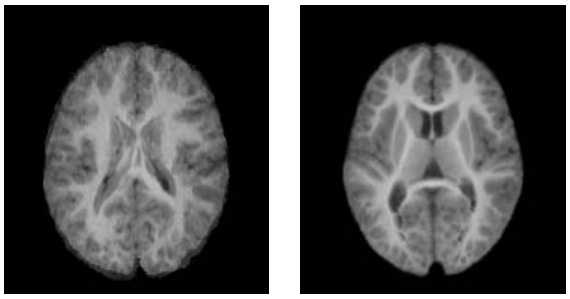

Fig. 4. Estimated templates initially and after 500 iterations

[1] Michael Miller, Ayananshu Banerjee, Gary Christensen, Sarang Joshi, Navin Khaneja, Ulf Grenander, and Larissa Matejic, "Statistical methods in computational anatomy," *Statistical Methods in Medical Research*, vol. 6, pp. 267–299, 1997.

[2] U. Grenander and M. I. Miller, "Computational anatomy: An emerging discipline," *Quarterly of Applied Mathematics*, vol. 56, pp. 617–694, 1998.

[3] P.M. Thompson, R.P. Woods, M.S Mega, and A.W Toga, "Mathematical/computational challenges in creating deformable and probabilistic atlases of the human brain," *Human Brain Mapping*, vol. 9, no. 2, pp. 81–92, Feb 2000.

[4] A. W. Toga, *Brain Warping*, Academic Press, San Diego, CA, 1999.

[5] I. Dryden and K. Mardia, *Statistical Shape Analysis*, John Wiley & Sons, New York, 1998.

[6] Michael I. Miller, Sarang C. Joshi, and Gary E. Christensen, "Large deformation fluid diffeomorphisms for landmark and image matching," in *Brain Warping*, Arthur W. Toga, Ed., chapter 7. Academic Press, 1999.

[7] M. I. Miller, A. Trouve, and L. Younes, "On the metrics and euler-lagrange equations of computational anatomy," *Annual Review of Biomedical Engineering*, vol. 4, pp. 375–405, 2002.

[8] Carole Twining, Stephen Marsland, and Chris Taylor, "Measuring geodesic distances on the space of bounded diffeomorphisms," in *BMVC2002*, P. L. Rosin and D. Marshall, Eds. BMVC, 2002.

[9] Peter Lorenzen and Sarang Joshi, "High-dimensional multmodal image registration," *Workshop on Biomedical Image Registration (WBIR)*, vol. LNCS-2717, pp. 234–243, 2003.

[10] Jianchun He and Gary E. Christensen, "Large deformation inverse consistent elastic image registration," in *IPMI3003, LNCS 2732*, C. J. Taylor and J. A. Noble, Eds. IPMI, 2003, pp. 438–449, Springer-Verlag.

[11] Gary E. Christensen, Richard D. Rabbitt, and Michael I. Miller, "Deformable templates using large deformation kinematics," *IEEE Transactions On Image Processing*, vol. 5, no. 10, pp. 1435–1447, October 1996.

[12] S. Joshi, P. Lorenzen, G. Gerig, and E. Bullitt, "Structural and radiometric asymmetry in brain images," *Medical Image Analysis*, vol. 7, no. 2, pp. 155–170, June 2003.